

1 **The contribution of tephra constituents during biogenic silica**
2 **determination: implications for soil and paleoecological studies**

3
4 Wim Clymans^{1,*}, Lúcia Barão², Nathalie Van der Putten¹, Stefan Wastegård³,
5 Guðrún Gísladóttir⁴, Svante Björck¹, Bertrand Moine⁵, Eric Struyf² and Daniel J.
6 Conley¹

7
8 ¹Department of Geology, Lund University, Sölvegatan 12, SE-22362 Lund,
9 Sweden

10 ²Department of Biology, Ecosystem Management, University of Antwerp,
11 Universiteitsplein 1, BE-2610 Wilrijk, Belgium

12 ³Department of Physical Geography, Stockholm University, SE-10691 Stockholm,
13 Sweden

14 ⁴Institute of Life and Environmental Sciences, and the Nordic Volcanological
15 Center, University of Iceland, Sturlugata 7, IS-101 Reykjavík, Iceland

16 ⁵Université de Lyon, Magmas et Volcans (UBP-UJM-CNRS-IRD), 23 rue Dr. P.
17 Michelon, F-42023 Saint-Etienne, France

18
19 *Corresponding author. Tel.: +46-4622-27888; fax: +46-4622-24830
20 *E-mail address:* wim.clymans@geol.lu.se

21
22 **Abstract**

23 Biogenic silica (BSi) is used as a proxy by soil scientists to identify biological
24 effects on the Si cycle and by paleoecologists to study environmental changes.
25 Alkaline extractions are typically used to measure BSi in both terrestrial and
26 aquatic environments. The dissolution properties of volcanic glass in tephra
27 deposits and their nano-crystalline weathering products are hypothesized to
28 overlap those of BSi, however, data to support this behavior are lacking. The
29 potential that Si-bearing fractions dissolve in alkaline media (Si_{Alk}) that do not
30 necessarily correspond to BSi, question the applicability of BSi as a proxy. Here,
31 analysis of 15 samples reported as tephra-containing allows us to reject the
32 hypothesis that tephra constituents produce an identical dissolution signal to
33 that of BSi during alkaline extraction. We found that dissolution of volcanic glass
34 shards is incomplete during alkaline dissolution. Simultaneous measurement of
35 Al and Si used here during alkaline dissolution provides an important parameter
36 to enable us to separate glass shard dissolution from dissolution of BSi and other
37 Si-bearing fractions. The contribution from volcanic glass shard (between 0.2-4
38 wt% SiO_2), the main constituent of distal tephra, during alkaline dissolution can
39 be substantial depending on the total Si_{Alk} . Hence, soils and lake sediments with
40 low BSi concentrations are highly sensitive to the additional dissolution from

41 tephra constituents and its weathering products. We advise evaluation of the
42 potential for volcanic or other non-biogenic contributions for all types of studies
43 using BSi as an environmental proxy.

44 **Keywords: Biogenic silica, Tephra, Alkaline extraction, Paleoecology,**
45 **Silicon cycle, Volcanic glass**

46 **1 Introduction**

47

48 Many plant and algae species take up dissolved silica (DSi) from the environment
49 and produce biogenic silica (BSi), a hydrated, amorphous SiO₂ polymorph that
50 provides structural and physiological benefits (Guntzer et al., 2012). BSi is
51 regularly estimated by soil scientists or paleoecologists using various alkaline
52 extraction techniques. These extraction techniques have supplanted other
53 methods in general usage, including microfossil counts (Leinen et al., 1985),
54 infrared spectroscopy (Meyer-Jacob et al., 2014) and X-ray diffraction. Each
55 technique has specific benefits and limitations (Ohlendurf and Storm, 2008). The
56 alkaline extraction techniques are applied to a range of environments and
57 archives, including soils, peat deposits, lake and marine sediments, wetland and
58 floodplain deposits and suspended matter in rivers (Andresen et al., 2004;
59 Clymans et al., 2011a; Clymans et al., 2011b; Cornelis et al., 2010; Fernández et
60 al., 2013; Frings et al., 2014b; Verschuren et al., 2002). In terrestrial ecosystems
61 vegetation may buffer DSi delivery to streams and rivers (Churchman and Lowe,
62 2012; Struyf and Conley, 2012). Hence, the magnitude of BSi accumulation in
63 soils is a key component in the biological buffering capacity of the Si cycle in an
64 ecosystem. Paleoecologists use BSi as a proxy for diatom productivity, and apply
65 this to infer changes in e.g. nutrient availability (Conley et al., 1993; Heathcote et
66 al., 2014), hydrology (Andresen et al., 2004), atmospheric circulation (Harper et
67 al., 1986; Johnson et al., 2011; Verschuren et al., 2002) and temperature (Adams
68 and Finkelstein, 2010; Prokopenko et al., 2006).

69

70 The methods vary in detail but all assume a difference in dissolution rate that
71 forms the basis of the separation of Si from mineral silicates and amorphous

72 biological fractions. Within the range of alkaline solutions used in the
73 experiments a fraction of the material may release Si at a slow and apparently
74 constant rate over the duration of the extraction (from here on referred to as a
75 'linearly dissolving fraction'). This corresponds to dissolution of mineral silicates
76 (Conley and Schelske, 2001; Koning et al., 2002). Some fractions may rapidly
77 release some or all of their Si within the duration of the extraction (from here on
78 'non-linearly dissolving fractions') and this non-linear fraction is conventionally
79 interpreted as the BSi fraction (DeMaster, 1981).

80

81 Unfortunately, various non-BSi fractions also release Si either completely or
82 partly in a non-linear manner in alkaline media, questioning the interpretation of
83 the non-linear part as biological in origin (Cornelis et al., 2011a; Gehlen and van
84 Raaphorst, 1993; Koning et al., 2002). Cornelis et al. (2011b) reviewed sources
85 that may completely dissolve and find that in addition to biogenic remains (e.g.
86 phytoliths, diatoms), inorganic forms such as Al-Si precipitates, volcanic glass
87 shards, adsorbed Si on amorphous Fe-oxides and nanocrystalline fractions such
88 as allophanes and imogolite, can comprise a substantial portion of the non-
89 linearly dissolving Si. Partial dissolution of clays can also rapidly release Si
90 (Barão et al., 2015; Koning et al., 2002). We introduce a procedural term 'Si_{Alk}'
91 (alkaline extracted Si) to refer to the full range of Si-bearing phases that dissolve
92 non-linearly under normal experimental conditions. It is becoming apparent that
93 Si_{Alk} does not necessarily correspond only to the BSi fraction, and thus caution is
94 warranted due to its implications for interpretation of the putative BSi record in
95 both soil and paleoecological studies.

96

97 Several studies have suggested that glass shards and their weathering products
98 (e.g. nanocrystalline minerals and secondary clays) could affect Si_{Alk}
99 measurements, as their dissolution characteristics in alkaline solutions can
100 overlap with the biogenic fraction (Barão et al., 2015; Hashimoto and Jackson,
101 1958; Sauer et al., 2006). Discrete volcanic ash deposits, composed of shards,
102 minerals together with pumice and rock fragments, known as tephra are
103 common in sedimentary archives; indeed, they form the basis of
104 tephrochronology (e.g. Lowe, 2011), a powerful technique for establishing age-

105 equivalence between sites. If dissolving glass (or mineral grain) in a tephra
106 releases Si in a similar way to BSi during dissolution in alkaline solutions, it has
107 the potential to make interpretation of Si_{Alk} difficult, since a change will not
108 uniquely represent a change in environmental conditions but also perhaps
109 periods of volcanic activity. Additionally, because of their often rapid dissolution,
110 glass, pumice, and other constituents in tephra can potentially induce elevated
111 DSi concentrations in lakes, causing shifts in phytoplankton communities (Lotter
112 et al., 1995; Hickman and Reasoner, 1994). Such a shift in the sedimentary
113 record may be incorrectly ascribed to a change in environmental conditions
114 providing a secondary indirect pathway to biased interpretations.

115

116 Here, we investigate volcanic glass shards and their weathering products as a
117 confounding factor during Si_{Alk} determination. We tested 1) dissolution
118 characteristics of glass in tephra deposits, and 2) whether tephra-derived
119 constituents contribute to Si_{Alk} measurements during alkaline extraction, and 3)
120 how such contributions affect the Si_{Alk} measurements in soils, sediments and
121 peats. We find that glass shards do not produce an identical dissolution signal to
122 that of BSi during alkaline extractions. However, the contribution of glass shards
123 to BSi can be substantial when low BSi concentrations are encountered in
124 environmental archives with important repercussions for soil and
125 paleoecological studies.

126 **2 Materials & Methods**

127 ***2.1 Tephra Samples***

128 Fifteen samples reported as tephra-containing and covering a representative
129 range of chemical composition (basaltic to rhyolitic), eruption dates (from 2010
130 AD until 48 ka BP), geographical provenance (northern and southern latitudes)
131 and environments (fresh deposits, soils, lakes and peat archives) have been
132 retrieved from archived samples (Table 1; Fig. 1). We used tephra collections
133 from tephra deposits described previously in soil and paleoecological studies
134 representing a gradient in weathering state.

135 **Table 1**

136 **2.2 Sample Treatment**

137 All samples were split in two parts to develop two distinct sample sets:
138 untreated *versus* treated. Untreated samples were immediately subjected to
139 alkaline extraction (section 2.3). The goal of treating samples is to isolate
140 relatively pure biogenic and volcanic glass derived fractions, which will allow us
141 to evaluate the robustness of the inferences made from the dissolution of the
142 untreated samples. Samples were subjected to standard pre-treatment and
143 heavy-liquid separation, described below, with additional magnetic separation
144 or sieving steps where necessary (Mackie et al., 2002; Morley et al., 2004;
145 Turney, 1998).

146 **Figure 1**

147 **2.2.1 Pre-treatment**

148 A 0.5-1 g subsample was weighed into a 15 ml centrifuge tube to which 30%
149 hydrogen peroxide (H₂O₂) was repeatedly added to remove organic matter at
150 80°C until reaction cessation. One millilitre of 10% HCl solution was added to
151 disaggregate the material and dissolve any soluble inorganics (e.g. carbonates)
152 and left until the reaction ceased. After each treatment step, the sample was
153 washed three times in deionized water (MilliQ).

154 **2.2.2 Heavy-liquid separation**

155 Heavy liquid separation is used to obtain concentrated siliceous organism
156 samples (i.e. diatoms and sponges) (Morley et al., 2004) and concentrated glass
157 shard samples (e.g. Turney, 1998). The biogenic part is concentrated by
158 centrifuging in sodium polytungstate (SPT) having a relative density of 2.3 g cm⁻³.
159 Prior to each centrifuge step, samples were thoroughly mixed, and if necessary
160 placed in an ultrasonic bath to disaggregate the material. The floating material (<
161 2.3 g cm⁻³) was dried (70°C) and assessed with SEM for purity, i.e. biogenic
162 material, or possible contamination from pumice and other non-biogenic light
163 fractions. The residue (>2.3 g cm⁻³) was centrifuged in SPT at a relative density of
164 2.5 g cm⁻³. Both floating material (between 2.3 g cm⁻³ and 2.5 g cm⁻³) and residue
165 (>2.6 g cm⁻³) were washed with MilliQ. The latter should contain heavy minerals,
166 and only a limited amount of glass shards, which should instead be concentrated

167 within the 2.3 to 2.5 g cm⁻³ bracket. All residues were microscopically checked
168 for their purity.

169

170 The separation only rarely resulted in high-purity end-products. Additional *ad*
171 *hoc* sample specific treatments were conducted to improve the separation. In
172 case of high concentration of low-density shards (e.g. pumice) within the
173 biogenic sample (<2.3 g cm⁻³), a wet-sieving step was used to separate the
174 biogenic siliceous bodies from shards. Size-distributions for each fraction were
175 determined using light microscopy (Nikon SMZ1500, x16) and the NIS-Elements
176 software for size measurements. The selected mesh size corresponded with the
177 point of minimum overlap. In case of basaltic tephra shards (i.e. > 2.7 g cm⁻³)
178 magnetic separation of the >2.6 g cm⁻³ (Mackie et al., 2002) was applied to
179 concentrate pure basaltic shards.

180 **2.3 Alkaline extraction techniques**

181 Two different alkaline extractions were used to determine the Si_{Alk} content and
182 dissolution characteristics of the untreated and the isolated tephra and biogenic
183 silica fractions of the treated samples: the sequential 0.1 M Na₂CO₃ and the
184 continuous 0.5 M NaOH method.

185 **2.3.1 Sequential wet-alkaline extraction method: 0.1 M Na₂CO₃**

186 The Na₂CO₃ extraction is a weak-base method developed by DeMaster (1981)
187 who described that while alumino-silicates release Si linearly over time, most BSi
188 dissolves completely within the first 2 hrs of the digestion. In our analysis
189 (Conley and Schelske, 2001), approximately 30 mg of dried sample (< 2 mm) was
190 mixed in 40 ml of 0.1 M Na₂CO₃ solution and digested for 5 hours at 85°C. A 0.5
191 ml aliquot was removed after 3, 4 and 5 hours and neutralized with 4.5 ml of
192 0.021 M HCl, before DSi determination by the automated molybdate-blue
193 method (Grasshoff et al., 1983) using a Smartchem 200 (AMS Systea) discrete
194 analyser. The Si_{Alk} was calculated by determining the intercept of the regression
195 between total extracted Si and extraction time. Extrapolating the Si release to the
196 intercept is assumed to correct for mineral dissolution of Si. To evaluate its
197 suitability to correct for mineral dissolution, the typical subsampling scheme
198 was prolonged to 24 hrs and additional 0.5 ml subsamples were taken at 9, 10

199 and 11 hrs and again at 20, 22 and 24 hrs, and diluted in 9.5 ml 0.010 M HCl
200 instead of 4.5 ml to obtain optimal dilution.

201 **2.3.2 Continuous extraction method: 0.5 M NaOH**

202 We applied a stronger NaOH (0.5 M) digestion protocol (Barão et al., 2014;
203 Koning et al., 2002) with continuous monitoring of the extracted Si and
204 aluminium (Al) concentration through time. Briefly, between 20 and 100 mg of a
205 sample was mixed with 180 ml of 0.5 M NaOH (pH = 13.7) in a stainless steel
206 vessel. The vessel was incubated in a water bath at a constant temperature of
207 85°C and continuously stirred with a rotor to obtain a homogeneous mixture.
208 The vessel was sealed to prevent evaporation. The extraction fluid was fed into a
209 Skalar continuous flow analyzer at 0.42 ml min⁻¹. Si and Al concentrations were
210 determined simultaneously using the spectrophotometric molybdate–blue
211 method for Si (Grasshoff et al., 1983) and lumogallion fluorescence for Al (Hydes
212 and Liss, 1976) for 30-40 minutes.

213 A simultaneous fit of dissolved Si and Al curves was performed using equation
214 (1).

215

$$216 \quad Si_t = \left(\sum_{x=1}^n Si_{Alk,x} \times (1 - e^{-k_x \times t}) \right) + b \times t \quad Al_t = \left(\sum_{x=1}^n \frac{Si_{Alk,x}}{Si:Al_x} \times (1 - e^{-k_x \times t}) \right) +$$
$$217 \quad \frac{b \times t}{Si:Al_{min}} \quad (1)$$

218

219 where Si_t and Al_t is the pool of extracted silica and aluminum at time t ($\mu\text{mol l}^{-1}$);
220 $Si_{Alk,x}$ is the total pool of Si_{Alk} ($\mu\text{mol l}^{-1}$) of fraction x ; k is a parameter that reflects
221 the non-linear reactivity of the sample (min^{-1}); b reflects the linear reactivity and
222 $Si:Al_x$ and $Si:Al_{min}$ represent their respective Si:Al ratios. The dissolution curves
223 of Si and Al were used to identify fractions based on their Si:Al ratios. This
224 principle was first applied by Koning et al. (2002) in marine sediment samples,
225 where almost all alkaline extracted Si has a biogenic source, overprinted by a low
226 $Si:Al_x$ component from clay minerals dissolution. They showed that some
227 fractions that would be considered as biogenic using linear phase extrapolation
228 (i.e. the sequential extraction, above) were actually clay contamination, based on
229 the low $Si:Al_x$ ratios (between 1 and 4) in these fractions. We hypothesize that
230 glass from tephra will resemble such behaviour because of their relatively high

231 Al content. The k-parameter reflects how fast a Si bearing fraction reaches
232 complete dissolution in an alkaline media, and depends on bonding strengths
233 and specific reactive surface areas. Here, relative differences of k-values between
234 modelled fractions are used to classify high and low reactive fractions in alkaline
235 media, where nanocrystalline and absorbed Si fractions are suggested to be
236 more rapidly released as compared to biogenic Si fractions (Barão et al., 2015).

237

238 The number of fractions (x) in the first order model was determined by
239 consecutively allowing an extra fraction to obtain an optimal model fit (i.e.
240 reducing the RMSE using the Solver function within Microsoft Excel).

241 **3 Results**

242 ***3.1 Sequential wet-alkaline extraction method – 0.1 M Na₂CO₃***

243 **Table 2**

244 Alkaline silica (Si_{Alk}) extracted from a total of 14 tephra-containing samples
245 (EFJ2010_1504 not included) based on the 3-5h mineral dissolution slope (wt%
246 SiO₂ h⁻¹) vary between 0.3 and 16.7 wt% SiO₂ with an average of 3.01 ± 3.91 wt%
247 SiO₂. Mineral dissolution slope ranges between 0.03 and 0.65 wt% SiO₂ h⁻¹ with
248 an average of 0.35 ± 0.21 wt% SiO₂ h⁻¹. This high standard deviation suggests
249 variability within samples, but is heavily influenced by two outliers (Reclus R₁
250 and Tuhua tephra); median Si_{Alk} and mineral dissolution slope are 1.56 wt% SiO₂
251 and 0.28 wt% SiO₂ h⁻¹, respectively.

252

253 The median Si_{Alk} using the 20-24h mineral dissolution slope was 3.63 wt% SiO₂
254 with a median slope of 0.12 wt% SiO₂ h⁻¹. A paired t-test (signed rank) showed
255 that both (corrected) Si_{Alk} concentrations and mineral dissolution slope differed
256 significantly between the 3-5hrs and the 20-24hrs sampling intervals.

257

258 There is a large variability in the shape of the curves in extracted Si through time
259 (Fig. 2). Some samples exhibit a continuously gently decreasing slope with time
260 (Fig. 2.a), while others show initial rapid dissolution followed by a steep linear
261 increase (Fig. 2.b), whereas others increase rapidly but are followed by no

262 increase or only a minimal increase in Si extracted with time (Fig. 2.c).
263 Numerically, we define this gradient through comparing the Si_{Alk} after 3-5hrs
264 with those obtained after 20-24hrs (Table 2): we observe respectively high (3.0-
265 7.1), medium (1.5-2.5) and low (1-1.8) ratios. Ideally, constant mineral
266 dissolution with no additional amorphous Si extracted after 3hrs would
267 correspond to a ratio of 1.

268 **Figure 2 & Figure 3**

269 **3.2 Continuous alkaline extraction method: 0.5 M NaOH**

270 **3.2.1 Curve decomposition**

271 Results of curve fitting the continuous monitored Si and Al data during the
272 extractions are presented in Table 3 and Figures 2 and 3. Si_{Alk} concentrations
273 vary between 0.27 and 23.4 wt% SiO_2 with an average of 4.54 ± 6.08 wt% SiO_2
274 and a median of 2.31 wt% SiO_2 . On average, but not always, these concentrations
275 are significantly higher than those measured during the Na_2CO_3 3-5 h extraction
276 (section 3.1; $p=0.0016$), but do not differ significantly with the Na_2CO_3 20-24 h
277 extraction ($p=0.1540$; non-parametric t-test). However, relative differences
278 between the NaOH and Na_2CO_3 3-5 h extraction can be up to factor 2-5, and
279 values tend to be lower (up to 10 times) than those measured during the Na_2CO_3
280 20-24 h extraction.

281

282 The shape of the dissolution curves suggests the presence of three distinct
283 dissolution patterns similar to using the Na_2CO_3 methodology. A first set of
284 curves show a gently decreasing slope with time, and limited contribution of Al
285 (Fig. 2d – Group 1). The second set of curves shows a rapid increase at the onset
286 for both Si and Al, and afterwards evolves towards a more linear increase (Fig. 2e
287 – Group 2). The final set is characterized by a rapid increase at the onset with
288 varying contributions of Al, but mostly an order of magnitude lower than
289 extracted Si concentrations with a near zero or high mineral dissolution slope
290 (Fig. 2f – Group 3).

291

292 Optimal fits of the model to predict the dissolution curve included between one
293 to three different Si_{Alk} fractions each with a specific k-parameter and Si to Al

294 ratio (Table 3). We used the number of non-linear fractions (first order - see
295 equation 1) and their Si:Al_x to group the samples (see discussion, Fig. 2d-f, and
296 Table 3). One group of samples exhibited one non-linear fraction that was
297 released slowly with a k between 0.05 and 0.5 min⁻¹. The linear dissolution is
298 responsible for the majority of the increase in Si and Al concentrations through
299 time. Si:Al_x ratios for both fractions are approximately equal and range between
300 3 and 5.

301

302 **Table 3**

303

304 A second group has two fractions that dissolve non-linearly. The non-linear
305 fractions evolve rapid ($k > 0.7 \text{ min}^{-1}$) and slow ($k < 0.5 \text{ min}^{-1}$), respectively,
306 towards complete dissolution. The Si:Al_x ratio of the slow fraction falls between 1
307 and 2.5. The rapid reaction releases typically more Al leading to low Si:Al ratios
308 (< 1). The Si:Al_{min} ratio of the linear fraction ranges between 1 and 3.5. Finally,
309 two fractions that dissolve non-linearly typify a third set of samples: a rapid ($k >$
310 0.7 min^{-1}) fraction with Si:Al_x mostly below 1 and a slow fraction ($k < 0.5 \text{ min}^{-1}$)
311 with Si:Al_x above 8. One exception (Reclus R₁) has three fractions but no mineral
312 fraction and differs by having two slow fractions instead of one.

313 **3.2.2 Validation of curve decomposition procedure**

314 Dissolution curves using 0.5 M NaOH for all concentrated shard samples
315 (rhyolitic: between 2.3 g cm⁻³ to 2.5 g cm⁻³; basaltic $> 2.5 \text{ g cm}^{-3}$) were best
316 approximated with a single non-linear fraction and a linear (i.e. mineral) fraction
317 indicating successful physical separation of shards (see Table 4). Mineral
318 dissolution contributions were typically large in total Si and Al release, being the
319 main source after on average 5 minutes of dissolution for Al release. The initial Si
320 and Al release appears to be faster than before the cleaning and separation
321 treatment. This is reflected in higher Si:Al_x ratios and k-values. One exception -
322 the Reclus R₁ sample - did not contain a retrievable amount of shards.

323

324 The BSi rich samples ($< 2.3 \text{ g cm}^{-3}$) were fitted with a single non-linear fraction in
325 absence of a linear fraction. The only exception is the Tuhua tephra where two

326 non-linear fractions with varying dissolution rate were fitted: defined as a rapid
327 (0.47) and slow (0.05) k. All Si:Al_x were higher than 100. The total extracted Si
328 content averaged on 72 ± 11 wt% SiO₂.

329

330 **Table 4**

331 **4 Discussion**

332 Earlier studies have hypothesized that volcanic glass shards substantially
333 contribute to measured Si_{Alk} (Cornelis et al., 2011b; Lyle and Lyle, 2002; Sauer et
334 al., 2006). In the following, we discuss the specific dissolution characteristics of
335 glass shards, during alkaline extraction and implications for soil and
336 paleoecological studies. We formulate guidelines for the use of alkaline
337 extraction techniques to determine BSi in soils and sediments prone to volcanic
338 glass inputs.

339 **4.1 Incomplete dissolution during digestion**

340 In theory, Si_{Alk} should be insensitive to the choice of aliquot times during Na₂CO₃
341 extraction, if the dissolution of minerals does not violate the two key
342 assumptions of the original protocol outlined by DeMaster (1981): (i) complete
343 dissolution of all Si_{Alk} fractions within three hours, and (ii) the mineral fraction
344 should exhibit linear behavior during the course of the dissolution experiment.
345 The linear behavior is assumed to be caused by minimal changes in reactive
346 surface area of crystalline minerals during dissolution in a weak base, e.g. 0.1 M
347 Na₂CO₃.

348 Higher Si_{Alk} concentrations (Table 2) and lower mineral dissolution slope values
349 after 20-24 h for our samples suggest a prolonged non-linear behavior. We
350 interpret this as evidence for incomplete dissolution of alkali extractable
351 fractions within the first 3 h of extraction. Complete dissolution of glass takes
352 considerably longer than 3 h causing Si_{Alk} to be underestimated when sub-
353 sampling only over the 3-5 h time period. In addition, a decrease in reactivity
354 during the 24 h extraction violates the second assumption. Our samples must
355 contain another fraction that violates the second assumption, and only reaches a

356 state of apparent linear dissolution after the 5 hour sampling.

357 We observe a gradient in the severity (high degree, medium degree and low
358 degree) of incomplete dissolution expressed as the deviation from an ideal Si_{Alk}
359 (22-24 h/3-5 h) ratio of 1. Samples were grouped according to their extent of
360 deviation from the ideal. Most samples are not newly formed pure volcanic
361 deposits but instead are a complex set of samples from lakes, soils and peat bogs
362 (Table 1). We suggest that the differences in the extent of dissolution and in their
363 dissolution curves represent variations in composition and abundance of
364 different Si_{Alk} sources. Unfortunately, the Na_2CO_3 method cannot define the
365 origin of the different Si_{Alk} fractions. This makes quantification of the
366 contribution of volcanic material to BSi impossible.

367

368 **4.2 Towards separation of the different fractions**

369 The use of Si:Al ratios using the continuous NaOH extraction methodology can
370 improve the interpretation of dissolution and uncertainty of the Si source (Barão
371 et al., 2014). NaOH should also be more efficient in dissolving all amorphous and
372 nanocrystalline material present (Müller and Schneider, 1993; Gehlen and van
373 Raaphorst, 1993). We combine dissolution parameters in NaOH with microscopy
374 to attribute specific dissolving or releasing fractions to our three defined groups
375 (see section 3.2.1 and Fig. 3).

376 **4.2.1 A shard signature**

377 Group 1 represents relatively pure tephra samples (Fig. 2a, d) where dissolution
378 of glass shards dominates. Our data suggests that glass shards release the
379 majority of Si and Al at a rapid and a constant rate during the time period (ca. 30
380 min) we monitor dissolution in NaOH. In contrast to Na_2CO_3 , the stronger NaOH
381 seems to obtain apparent linear dissolution within the course of the experiment,
382 after an initial non-linear release. This initial decrease in reactivity followed by a
383 substantial constant Si and Al release corroborates previous observations
384 describing the stoichiometric dissolution of glass shards (Oelkers and Gislason,
385 2001; Stephens and Hering, 2004). Si:Al ratios of the non-linear Si_{Alk} and linear
386 fraction coincide with Si:Al ratios from unweathered glass shards ($\text{Si:Al}_{\text{Solid}}$). Si:Al

387 ratios of the pure tephra samples (presumably mainly glass) are plotted along
388 the 1:1 line demonstrating stoichiometric behavior (Fig. 4a).

389

390 Oelkers and Gisslasson (2001) delivered a theoretical framework for volcanic
391 glass shard dissolution at acidic and alkaline conditions that adequately
392 describes our observed dissolution patterns in both Na_2CO_3 and NaOH solutions.
393 Initially, proton exchange reactions will lead to the removal of univalent and
394 divalent cations from the shard surfaces, followed by a partial removal of Al from
395 the framework through the same process. Finally, Si liberation is possible
396 through the weakened state of Si as it is present in Si tetrahedrals, i.e. only
397 partially attached to the framework by only one or two bridging oxygen atoms
398 primarily located at the edges and tips of the shard. As smoothing of the
399 shards progresses, and depending on the abundance of hydrated sites, the
400 weakened state of Si at the edges can lead to faster release of Si at the onset,
401 which decreases as the edges become rounded. The rounding of edges is
402 responsible for the observed Si_{Alk} content when glass shards are dissolved.
403 Afterwards, glass shards will continue to release Si and Al at a steady
404 stoichiometric rate (see also Hodder et al., 1990). Hence, the dissolution pattern
405 reflects the continuous but incomplete dissolution of glass shards. This process
406 makes the dissolution of glass shards distinct from the dissolution of other non-
407 biogenic (e.g. nanocrystalline minerals) or biogenic fractions and adsorbed Si
408 and Al release. These processes occur rapidly at the onset of NaOH extraction but
409 do not lead to a fast constant release after unspecified time (Barão et al., 2014;
410 Hashimoto and Jackson, 1958).

411

412 Based on the pure samples of tephra (i.e. glass rich), we suggest that shards have
413 a distinct dissolution signature discernable using continuous monitoring during
414 a 0.5 M NaOH extraction. The three defining characteristics are: 1) the mineral
415 dissolution slope is extremely high ($0.028\text{-}0.120 \text{ wt}\% \text{ SiO}_2 \text{ min}^{-1}$) with 2) a Si:Al
416 ratio in the extracted aqueous phase between 3 and 5 equal to that of un-
417 weathered shards confirming stoichiometric dissolution and its volcanic origin,
418 and 3) a slow non-linear fraction with $(\text{Si}:\text{Al}_{\text{aq}} / \text{Si}:\text{Al}_{\text{solid}}) = \pm 1$ indicates an initial
419 stoichiometric dissolution until edges are rounded (Table 3; Fig. 4). Re-analysis

420 with the NaOH method of isolated glass shards is consistent with a constant and
421 stoichiometric dissolution of shards with time (Fig 5b). Unfortunately, chemical
422 pre-treatment with HCl and H₂O₂ has affected the dissolution characteristics of
423 the shards creating an initial more rapid release of Si and Al.

424

425 We propose that acidic conditions during the cleaning procedure lead to partial
426 dissolution of the volcanic glass shards as shown by Wolff-Boenisch et al. (2004)
427 in acidic and far-from-equilibrium conditions for a range of shards (low and high
428 SiO₂ content). The process at acid conditions can be equally described as for
429 alkaline solutions through the two phase process of deprotonation of Al followed
430 by liberation of Si (Oelkers and Gislason, 2001). However, Al is preferentially
431 released due to the formation of a silica gel layer at pH < 9 with a thickness
432 depending on the exposure time to acids (Pollard et al., 2003). Of course,
433 addition to an alkaline environment led to a rapid dissolution of any enriched
434 silica gel coating. This provides an explanation for the high Si:Al_x ratios and rapid
435 Si release rates after pre-treatment (Table 4). We advise against chemical pre-
436 treatment when analyzing for BSi, because it causes the extraction of non-
437 biogenic fractions.

438

439 **4.2.2 Discerning a shard signature from non-biogenic Si_{Alk}**

440 In group 2 and 3 (Fig. 2), multiple non-linear fractions were observed when
441 modeling dissolution curves. We attribute the contribution of shards to the Si_{Alk}
442 fraction that evolves slowest to constant release (i.e. lowest k) while a low Si:Al_x
443 ratio suggests a non-biogenic source for the more rapid second Si_{Alk} fraction.

444

445 Group 2 and 3 are samples from lake, soil and peat records. Here, shards are
446 mixed with a variety of materials during deposition including organic carbon,
447 minerals and siliceous organisms. The tephra samples with the highest
448 contribution of the secondary Si_{Alk} fraction (e.g. Katla, Reykjanes, Saksunarvatn,
449 basaltic part of the Vedde Ash) have a lower stability according to Pollard's
450 theoretical stability modeling (2003). Likewise, the Parker index value for the
451 Tuhua tephra indicates a higher propensity for rapid weathering (Lowe, 1988).

452 We suggest that enhanced weathering in these environments leads to the
453 formation of secondary mineral and nanocrystalline fractions (Hodder et al.,
454 1990). This would create an additional non-biogenic, alkaline extractable source.
455 Such weathering products are typically enriched in Al with structural Si:Al_x
456 ratios between 1-3 for clay minerals (Dixon and Weed, 1989) and below 1 for
457 nanocrystalline structures (Levard et al., 2012). In fact, they dissolve or release
458 Si and Al more rapidly, and sometimes incongruently, at the beginning of a NaOH
459 extraction (Hashimoto and Jackson, 1958; Koning et al., 2002). This explains why
460 we observe a large range in Si:Al_x ratios (0.5-4) initially during the extraction.
461 We suggest it either represents the non-linear part of clay dissolution (Si:Al_x
462 ratio: 1-4) or complete dissolution of nanocrystalline minerals (Si:Al_x ratio: 0.5-
463 1).

464

465 Clay minerals will dissolve at a constant rate after an initial rapid release
466 (Koning et al., 2002) similar to primary glass shards. Consequently, the linear
467 part of the dissolution will reflect stoichiometric dissolution of glass shards
468 (Si:Al_{min} ratio: 3-5) and clay minerals (Si:Al_{min} ratio: 1-3). Samples with increased
469 abundance of clay contribution will have lowered Si:Al_{min} ratios compared to un-
470 weathered shards (Fig. 4.a).

471

472 **4.2.3 Discerning a shard signature from biogenic Si_{Alk}**

473 In group 3, higher Si:Al_x ratios > 5 for the slower fraction suggest the presence of
474 an additional biogenic Si_{Alk} fraction. Biogenic fractions including diatoms, sponge
475 spicules and phytoliths were identified in these samples microscopically. BSi
476 measurements of the separated biogenic fraction using the continuous NaOH
477 methodology had a single non-linear Si_{Alk} fraction, except Tuhua, with on average
478 72 wt% SiO₂. This fraction contains negligible amounts of Al and mineral
479 dissolution is absent confirming the biogenic nature of the separated material.
480 The combined presence of diatoms and sponge spicules in the Tuhua samples
481 explains the observation of two distinct BSi fractions (based on reactivity), as
482 alkaline dissolution rates are known to vary between different siliceous
483 organisms (Conley and Schelske, 2001).

484

485 Hence, it seems that the rounding of glass shards overlaps with the dissolution of
486 biogenic material, having similar reactivity but higher Si:Al_x ratios. The distinct
487 pattern of pure shards can be used to make a minimum estimate of its
488 contribution to the slower reacting fraction. Identification of glass shards'
489 dissolution behavior is essential to evaluate the methods ability to estimate the
490 biogenic Si_{Alk} content and evaluate the relative contribution of shard dissolution
491 to Si_{Alk}. The separation is based on the near to one ratio between Si:Al_x with the
492 Si:Al_{Solid} (Fig. 4).

493

494 **Figure 5**

495

496 Assumption 1: Si:Al corresponding to the slow fraction (Si_{Alk,1}) equals the Si:Al of
497 shards

498

OR

$$\left(\frac{Si}{Al}\right)_1 \approx \left(\frac{Si}{Al}\right)_{Solid}$$

499

500

501 Assumption 2: All Al originates from shards for the slow fraction i.e. no Al release
502 from the biogenic fraction. This leads to an overestimation of Al as small
503 amounts (< 0.05 wt%) of Al are found in phytoliths and diatoms (Kameník et al.,
504 2013; Van Cappellen et al., 2002).

505

$$Al_1 = Al_{Bsi} + Al_{Solid} \text{ with } Al_{Bsi} = 0$$

506 So,

$$Al_1 = Al_{Solid}$$

507

508 The Si coming from shards can then be calculated by substitution:

$$Si_{Solid} = \left(\frac{Si}{Al}\right)_{Solid} \cdot Al_1$$

509

510 We know that,

511

$$Si_1 = Si_{BSi} + Si_{Solid}$$

512 This delivers:

$$Si_{BSi} = Si_1 - Si_{Solid}$$

513

514 The results of this separation exercise combined with the observed difference in
515 other fractions are provided in Figure 5. Significant shards contribution to Si_{Alk} is
516 observed for all samples except Reclus R₁. Although we have no definitive
517 explanation why our Reclus R₁ sample did not contain observable amounts of
518 shards, our results support the physical observation of no retrievable shard
519 fraction by heavy liquid separation. If anything, it supports the appropriateness
520 of the chemical analysis to detect the occurrence of shards.

521

522 Initial dissolution of shard edges varies between 0.1 to 8 wt% SiO₂ with a median
523 contribution of 1.8 wt% SiO₂. The variation in contribution depends on how
524 fragmented and weathered (i.e. partially dissolved) the glass shards are. There
525 will be a decrease in its contribution if edges have been smoothed during natural
526 dissolution processes. It shows that dissolution of glass shards can contribute
527 substantially to the determination of BSi when BSi concentrations are low.
528 Likewise, the non-biogenic Si sources (defined as “minerals” here) contribute
529 between 0.2 to 5 wt% SiO₂ with a median contribution equal to 0.89 wt% SiO₂.
530 The combined effect potentially exceeds the biogenic fraction (e.g. K1500), while
531 for others it contributes to less than 10% of the total extracted Si pool (e.g.
532 Armor1000 and Reclus R₁).

533

534 ***4.3 The tephra factor in soil and paleoecological studies***

535 **4.3.1 Implications for soil scientists**

536 The global median Si_{Alk} in the top 1m of the soil column using alkaline extraction
537 techniques ranges between 0.79-1.12 wt% SiO₂ (e.g. Melzer et al., 2012; Saccone
538 et al., 2007; Sommer et al., 2013). The magnitude overlaps with Si_{Alk} content
539 attributed to tephra, to the initial rapid dissolution of clay minerals and/or
540 complete dissolution of nanocrystalline fractions in our experiments (Fig. 5). A

541 similar magnitude of Si release between soil samples and our untreated tephra
542 samples during alkaline extraction, implies that the combined dissolution of
543 glass shards, and their weathering products, if present, can disguise for a limited
544 amount of settings the environmental signal of the BSi proxy.

545

546 Glass shards are an important direct source of methodological bias in tephra-
547 based soils, that include Andosols (ISSS-ISRIC-FAO, 1998). Andosols have a
548 limited spatial extent covering about 1-2% of the land surface. Likewise, volcanic
549 bedrock formed at the surface covers 6.6% of the land surface (Hartmann and
550 Moosdorf, 2012) and is known to contain limited amounts of glass shards, which
551 are a potential source of Si_{Alk} in soils. Further, glass shards can be an important
552 component of soils developed in aeolian deposits in the Great Plains, USA
553 (Reyerson, 2012). The inheritance of glass shards in some types of aeolian
554 material might partly explain high Si_{Alk} in aeolian deposits measured by other
555 studies (e.g. 4 wt% SiO_2 ; Saccone et al., 2007).

556

557 Better knowledge of the mineralogical composition of our samples could
558 improve classification of the non-biogenic fractions. Weathering products of
559 glass shards are proposed to be the largest contributor to the Si_{Alk} fraction. A
560 Si:Al_x ratio between 0.39 and 1.02 (5 out of 8 samples) for this fraction suggest
561 its source to be nanocrystalline fractions. These fractions are typically described
562 as allophanes and imogolites with a Si:Al_x ratio between 0.5-1 (Levard et al.,
563 2012), and dissolve completely within the first 5 minutes of alkaline extraction
564 (Hashimoto and Jackson, 1958; Kamatani and Oku, 2000). Various studies have
565 shown that these nanocrystalline minerals also develop in soils without a
566 volcanic origin (Gustafsson et al., 1999; Parfitt, 2009). For example, in podzols
567 supersaturation of Al species at ambient dissolved Si concentration leads to the
568 formation of allophanes and imogolites. Nanocrystalline structures are stable at
569 ambient pH conditions above 5 (Parfitt, 2009). Extraction of Si_{Alk} will include
570 them in the biological pools (Clymans et al., 2014) and lead to an overestimation
571 of BSi in both volcanic and non-volcanic soils at ambient pH conditions.

572

573 We recommend caution when interpreting Si_{Alk} measurements from Andosols, or
574 soils developed on volcanic bedrock, at sites where inheritance of volcanic
575 material through aeolian or water deposition is likely. The NaOH method (after
576 Koning et al., 2002) proved its ability to pinpoint problematic samples, and to
577 separate the biogenic from non-biogenic fractions. The method delivers an
578 excellent opportunity to improve the determination of BSi pools in soil profiles.

579 **4.3.2 Implications for paleoecological studies**

580 Biogenic silica, estimated as Si_{Alk} , has proven to be a valuable tool in
581 paleoecological studies as an indicator of environmental changes (e.g. changes in
582 productivity, climate, precipitation and nutrient supply). In lacustrine sediment
583 cores, BSi content can range from the detection limit (0.01 wt%) to >70 wt%
584 SiO_2 (Frings et al., 2014a). The downcore variations in BSi through time vary
585 from as little as 2 wt% SiO_2 (Adams and Finkelstein, 2010; Ampel et al., 2008) to
586 a high of 10-40 wt% SiO_2 (Johnson et al., 2011; Prokopenko et al., 2006; Van der
587 Putten et al., 2015) and depends on several interacting factors such as mineral
588 matter or organic matter accumulation, diatom productivity and
589 preservation/dissolution processes. Hence, these processes control the relative
590 effect that tephra constituents (<3 wt% SiO_2 , Fig. 5) have on Si_{Alk} determination.
591 In paleorecords, where there is a potential contribution of tephra combined with
592 low Si_{Alk} concentrations or small downcore variations in Si_{Alk} , the use of Si_{Alk} as
593 an environmental proxy should be used with caution.

594

595 The accuracy of the alkaline extraction methods as a proxy for BSi
596 concentrations in sediment will depend on the origin of the mineral matter.
597 Koning et al. (2002) suggested that good results with the NaOH method can be
598 obtained for BSi/clay ratios of about 0.005, whereas for Na_2CO_3 good values can
599 be obtained from a 0.02 ratio. We show that for tephra samples it is a bit more
600 complicated as rounding of the glass shards edges and dissolution of its
601 weathering products (i.e. nanocrystalline minerals and secondary minerals) also
602 contribute to the apparent BSi fraction. Obviously, the spatial and therefore
603 temporal extent of potential contribution is restricted to core sections
604 representing episodes of 1) direct tephra deposition, and subsequent in-situ

605 reworking; or 2) indirect contribution through mobilization of tephra and its
606 weathering products in a tephra covered landscape.

607

608 Our study highlights a direct effect of tephra on quantification of BSi.
609 Additionally, tephra deposition in lakes and peatlands can alter the diatom
610 community composition and diatom abundance (Harper et al., 1986; Hickman
611 and Reasoner, 1994; Lotter et al., 1995), though not always (Telford et al., 2004).
612 Tephra input can induce a change in water chemistry, causing altered diatom
613 growth and/or preservation (for a review see Harper et al., 1986). In such case,
614 the increase in BSi accumulation can be indirectly attributed to tephra
615 deposition rather than to environmental changes. The methods used in our study
616 cannot distinguish between tephra induced diatom blooms and those resulting
617 from short- or long-term environmental change. Nevertheless, zones in a
618 sediment record potentially prone to a tephra-induced bloom can be highlighted
619 based on reconnaissance of glass shard contributions. This research topic
620 warrants further investigation, and requires detailed analysis of high resolution
621 records known to be prone to volcanic inputs.

622

623 **4.3.3 Implications for pre-treatment steps of EPMA during** 624 **tephrochronological studies**

625 Tephrochronology requires geochemical fingerprinting of tephra through
626 electron probe microanalysis (EPMA) (Lowe, 2011). EPMA on tephra requires
627 that they are unaltered by natural or laboratory processes. Unfortunately, tephra
628 shards are sensitive to dissolution at high and low pH, conditions that are both
629 naturally occurring and frequently applied during pre-treatment (e.g. Blockley et
630 al., 2005; Dugmore et al., 1992). Therefore, corrosive chemical pre-treatment is
631 increasingly avoided in tephrochronological studies and has been replaced by
632 heavy liquid floatation protocols (Blockley et al., 2005; Turney, 1998). The use of
633 NaOH (typical 0.3M in tephra preparation studies) for cleaning tephra samples of
634 biogenic Si (Davies et al., 2003; Rose et al., 1996; Wulf et al., 2013) should be
635 used with great caution. Our study demonstrates that alkaline treatments lead to
636 severe dissolution of shards, and can negatively affect the reconnaissance of
637 shards for EPMA analysis. Our data show that dissolution of the shards was

638 equivalent to 4 wt% SiO₂ in the first 40 minutes (Fig. 2.a) and that a complete
639 dissolution is attained in less than a day. The severity of the dissolution effect
640 depends on the duration of extraction, the temperature at which extraction is
641 performed and the molarity of the solution used (Müller and Schneider, 1993).
642 Good criteria for NaOH cleaning are that extraction times should 1) allow
643 complete BSi dissolution, and 2) limit shard dissolution to a maximum of 10 wt%
644 SiO₂ so that a sufficient number of undamaged shards remain for EPMA analysis.
645 Finally, the Si and Al data suggest stoichiometric dissolution of shards implying
646 that their geochemical composition will remain unaltered. We cannot be
647 conclusive as modeled Si:Al are too imprecise and the release of other dominant
648 constituents (e.g. Na, K) were not monitored. EPMA on samples before and after
649 alkaline treatment (preferentially NaOH) could resolve this issue.

650 **5 Conclusion**

651 Various wet chemical alkaline extraction techniques commonly used to measure
652 Si_{Alk} content have been criticized for their usefulness outside marine sciences.
653 Problems are attributed to dissolution of non-biogenic fractions and incomplete
654 dissolution of the biogenic fraction. We evaluated two alkaline extraction
655 techniques using 0.1 M Na₂CO₃ and 0.5 M NaOH solutions for measuring Si_{Alk} as a
656 proxy for environmental change in soil, peat and lake records with volcanic
657 inputs.

658

659 Alkaline extraction techniques should be used with caution in tephra-based soil
660 profiles, soils developed on volcanic bedrock or soils with aeolian input
661 containing volcanic material. The influence of the dissolution of glass shards on
662 BSi measurements in paleoecological records can be significant in oligotrophic
663 environments with a low BSi sediment content. Here, concomitant accumulation
664 of volcanic material will lead to significant contribution of a non-biogenic
665 fraction during the determination of Si_{Alk}. Otherwise, Si_{Alk} determined with
666 traditional alkaline methods can be freely used as a proxy to evaluate
667 environmental changes, especially when part of multi-proxy studies.

668

669 Determination of the time course of dissolution during the first 5 hours of
670 extraction using 0.1 M Na₂CO₃ has proven to be a sensitive indicator of other
671 forms of Si_{Alk}. In addition, the sequential Na₂CO₃ extraction is a rather simple
672 method and the results show a high recovery of the biogenic Si fraction (Meunier
673 et al., 2014; Saccone et al., 2007). The main advantage of the method is that a
674 relatively large number of samples can be measured in a relatively short time
675 span. In environments with a high BSi content, the 0.1 M Na₂CO₃ method is the
676 preferred one.

677

678 We also show that the continuous monitoring of Si and Al extraction in NaOH
679 addresses the main disadvantages of the sequential Na₂CO₃ method. Our analysis
680 of pure tephra (i.e. mainly containing glass shards) samples provided important
681 information about the dissolution characteristics of volcanic glass shards. Our
682 study confirms that the dissolution of tephra contributes to Si_{Alk} determination,
683 but the distinct signature of glass shard dissolution can help to isolate its
684 contribution to the biogenic fraction. Continuous monitoring of Si and Al is
685 promoted to analyze complex samples from any environmental record to reduce
686 uncertainty on biological reactive fractions. Future studies should address the
687 reliability and precision of the separation of different fractions through modeling
688 of dissolution parameters.

689

690 **Acknowledgments:**

691 The following people are thanked for their invaluable assistance: S.R. Gíslason
692 for providing fresh tephra (Eyjafjallajökull). A. Cools, D.U. Delmonte for
693 assistance during the continuous extractions. A. Gosh helping with microscopic
694 analysis. G. Fontorbe, P. Abbott, S. Davies for advice on sample preparation.
695 Comments by P. Frings, G. Fontorbe, H. Alfredsson, B. Alvarez de Glasby, and J.
696 Stadmark improved the manuscript. Likewise, the editor, anonymous reviewers
697 and D.J. Lowe are thanked for their constructive comments and suggestions. This
698 research was funded by the Knut & Alice Wallenberg Foundation, FWO en Belspo
699 (SOGLO). LB thanks Special Research Funding from the University of Antwerp
700 (BOF-UA and NOI) for the PhD fellowship funding.

701

702 **Author contributions:**

703 WC, NVdP, DJC were responsible for the concept and design of this study. SW, SB,
704 NVdP, BM and GG advised on, and helped with sample collection. WC, LB and
705 NVdP prepared and analyzed samples. WC was responsible for data analysis and
706 interpretation with inputs on methodology of LB, ES and DJC, and interpretation
707 of paleoecological data by all other authors. WC provided a first draft. All authors
708 contributed to the writing of the paper.

709

710

711

712 **References:**

713 Adams, J. K., and Finkelstein, S. A.: Watershed-scale reconstruction of middle and
714 late Holocene paleoenvironmental changes on Melville Peninsula, Nunavut,
715 Canada, *Quaternary Sci Rev*, 29, 2302-2314, 10.1016/j.quascirev.2010.05.033,
716 2010.

717 Ampel, L., Wohlfarth, B., Risberg, J., and Veres, D.: Paleolimnological response to
718 millennial and centennial scale climate variability during MIS 3 and 2 as
719 suggested by the diatom record in Les Echets, France, *Quaternary Sci Rev*, 27,
720 1493-1504, 10.1016/j.quascirev.2008.04.014, 2008.

721 Andresen, C. S., Björck, S., Bennike, O., and Bond, G.: Holocene climate changes in
722 southern Greenland: evidence from lake sediments, *J Quaternary Sci*, 19, 783-
723 795, 10.1002/jqs.886, 2004.

724 Barão, L., Clymans, W., Vandevenne, F., Meire, P., Conley, D., and Struyf, E.:
725 Pedogenic and biogenic alkaline - extracted silicon distributions along a
726 temperate land - use gradient, *Eur J Soil Sci*, 65, 693-705, 2014.

727 Barão, A., Vandevenne, F., Clymans, W., Frings, P., Ragueneau, O., Meire, P.,
728 Conley, D. J., and Struyf, E.: Alkaline-extractable silicon from land to ocean: a
729 challenge for biogenic Silicon determination, *Limnology and Oceanography*:
730 *Methods*, In press, 2015.

731 Björck, S., Rittenour, T., Rosén, P., França, Z., Möller, P., Snowball, I., Wastegård, S.,
732 Bennike, O., and Kromer, B.: A Holocene lacustrine record in the central North
733 Atlantic: proxies for volcanic activity, short-term NAO mode variability, and long-
734 term precipitation changes, *Quaternary Sci Rev*, 25, 9-32,
735 <http://dx.doi.org/10.1016/j.quascirev.2005.08.008>, 2006.

736 Blockley, S. P. E., Pyne-O'Donnell, S. D. F., Lowe, J. J., Matthews, I. P., Stone, A.,
737 Pollard, A. M., Turney, C. S. M., and Molyneux, E. G.: A new and less destructive
738 laboratory procedure for the physical separation of distal glass tephra shards
739 from sediments, *Quaternary Sci Rev*, 24, 1952-1960,
740 10.1016/j.quascirev.2004.12.008, 2005.

741 Churchman, J., and Lowe, D. J.: Alteration, formation, and occurrence of minerals
742 in soils, 2nd ed., *Handbook of Soil Sciences. Vol. 1: Properties and Processes*,
743 edited by: Huang, P., and Li, Y., CRC Press, 2012.

- 744 Clymans, W., Govers, G., Van Wesemael, B., Meire, P., and Struyf, E.: Amorphous
745 silica analysis in terrestrial runoff samples, *Geoderma*, 2011a.
- 746 Clymans, W., Struyf, E., Govers, G., Vandevenne, F., and Conley, D. J.:
747 Anthropogenic impact on amorphous silica pools in temperate soils,
748 *Biogeosciences*, 8, 2281-2293, 10.5194/bg-8-2281-2011, 2011b.
- 749 Clymans, W., Lehtinen, T., Gísladóttir, G., Lair, G., Barão, L., Ragnarsdóttir, K.,
750 Struyf, E., and Conley, D.: Si Precipitation During Weathering in Different
751 Icelandic Andosols, *Procedia Earth Planet Sci*, 10, 260-265, 2014.
- 752 Conley, D., Schelske, C., and Stoermer, E.: Modification of the biogeochemical
753 cycle of silica with eutrophication, *Mar Ecol Prog Ser*, 101, 179-192, 1993.
- 754 Conley, D., and Schelske, C.: Biogenic silica, in: *Tracking Environmental Change
755 Using Lake Sediments: Biological Methods and Indicators*, edited by: Smol, J.,
756 Birks, H., and Last, W., Kluwer Academic Press, 281-293, 2001.
- 757 Cornelis, J.-T., Titeux, H., Ranger, J., and Delvaux, B.: Identification and
758 distribution of the readily soluble silicon pool in a temperate forest soil below
759 three distinct tree species, *Plant Soil*, 342, 369-378, 10.1007/s11104-010-0702-
760 x, 2011a.
- 761 Cornelis, J. T., Ranger, J., Iserentant, A., and Delvaux, B.: Tree species impact the
762 terrestrial cycle of silicon through various uptakes, *Biogeochemistry*, 97, 231-
763 245, 10.1007/s10533-009-9369-x, 2010.
- 764 Cornelis, J. T., Delvaux, B., Georg, R. B., Lucas, Y., Ranger, J., and Opfergelt, S.:
765 Tracing the origin of dissolved silicon transferred from various soil-plant
766 systems towards rivers: a review, *Biogeosciences*, 8, 89-112, 2011b.
- 767 Davies, S. M., Wastegård, S., and Wohlfarth, B.: Extending the limits of the
768 Borrobol Tephra to Scandinavia and detection of new early Holocene tephtras,
769 *Quaternary Res*, 59, 345-352, 2003.
- 770 DeMaster, D.: The supply and accumulation of silica in the marine-environment,
771 *Geochim Cosmochim Acta*, 45, 1715-1732, 1981.
- 772 Dixon, J. B., and Weed, S. B.: *Minerals in soil environments*, 2nd ed., Minerals in
773 soil environments, Soil Sci Soc Am J, Madison, Wisconsin, USA, 1989.
- 774 Dugmore, A. J., Newton, A. J., Sugden, D. E., and Larsen, G.: Geochemical stability
775 of fine-grained silicic Holocene tephra in Iceland and Scotland, *J Quaternary Sci*,
776 7, 173-183, 10.1002/jqs.3390070208, 1992.
- 777 Fernández, M., Björck, S., Wohlfarth, B., Maidana, N. I., Unkel, I., and Van der
778 Putten, N.: Diatom assemblage changes in lacustrine sediments from Isla de los
779 Estados, southernmost South America, in response to shifts in the southwesterly
780 wind belt during the last deglaciation, *J Paleolimnol*, 50, 433-446,
781 10.1007/s10933-013-9736-4, 2013.
- 782 Frings, P., Clymans, W., Jeppesen, E., Lauridsen, T., Struyf, E., and Conley, D.: Lack
783 of steady-state in the global biogeochemical Si cycle: emerging evidence from
784 lake Si sequestration, *Biogeochemistry*, 117, 255-277, 10.1007/s10533-013-
785 9944-z, 2014a.

786 Frings, P. J., Clymans, W., and Conley, D. J.: Amorphous Silica Transport in the
787 Ganges Basin: Implications for Si Delivery to the Oceans, *Procedia Earth Planet*
788 *Sci*, 10, 271-274, 2014b.

789 Gehlen, M., and van Raaphorst, W.: Early diagenesis of silica in sandy North sea
790 sediments: quantification of the solid phase, *Mar Chem*, 42, 71-83,
791 [http://dx.doi.org/10.1016/0304-4203\(93\)90238-J](http://dx.doi.org/10.1016/0304-4203(93)90238-J), 1993.

792 Gísladóttir, G., Erlendsson, E., Lal, R., and Bigham, J.: Erosional effects on
793 terrestrial resources over the last millennium in Reykjanes, southwest Iceland,
794 *Quaternary Res*, 73, 20-32, <http://dx.doi.org/10.1016/j.yqres.2009.09.007>,
795 2010.

796 Gislason, S. R., Alfredsson, H. A., Eiríksdóttir, E. S., Hassenkam, T., and Stipp, S. L.
797 S.: Volcanic ash from the 2010 Eyjafjallajökull eruption, *Appl Geochem*, 26, S188-
798 S190, [10.1016/j.apgeochem.2011.03.100](http://dx.doi.org/10.1016/j.apgeochem.2011.03.100), 2011a.

799 Gislason, S. R., Hassenkam, T., Nedel, S., Bovet, N., Eiríksdóttir, E. S., Alfredsson, H.
800 A., Hem, C. P., Balogh, Z. I., Dideriksen, K., Oskarsson, N., Sigfusson, B., Larsen, G.,
801 and Stipp, S. L.: Characterization of Eyjafjallajökull volcanic ash particles and a
802 protocol for rapid risk assessment, *P Natl Acad Sci USA*, 108, 7307-7312,
803 [10.1073/pnas.1015053108](http://dx.doi.org/10.1073/pnas.1015053108), 2011b.

804 Grasshoff, K., Ehrhardt, M., and Kremling, K.: *Methods of Sea Water Analysis*, 314,
805 1983.

806 Gudmundsson, A., Oskarsson, N., Grönvold, K., Saemundsson, K., Sigurdsson, O.,
807 Stefansson, R., Gislason, S., Einarsson, P., Brandsdóttir, B., Larsen, G.,
808 Johannesson, H., and Thordarson, T.: The 1991 eruption of Hekla, Iceland, *B*
809 *Volcanology*, 54, 238-246, [10.1007/BF00278391](http://dx.doi.org/10.1007/BF00278391), 1992.

810 Guntzer, F., Keller, C., and Meunier, J.-D.: Benefits of plant silicon for crops: a
811 review, *Agron Sustain Dev*, 32, 201-213, 2012.

812 Gustafsson, J. P., Bhattacharya, P., and Karlton, E.: Mineralogy of poorly
813 crystalline aluminium phases in the B horizon of Podzols in southern Sweden,
814 *Appl Geochem*, 14, 707-718, [http://dx.doi.org/10.1016/S0883-2927\(99\)00002-](http://dx.doi.org/10.1016/S0883-2927(99)00002-5)
815 [5](http://dx.doi.org/10.1016/S0883-2927(99)00002-5), 1999.

816 Hafliðason, H., Larsen, G., and Ólafsson, G.: The Recent Sedimentation History of
817 Thingvallavatn, Iceland, *Oikos*, 64, 80-95, [10.2307/3545044](http://dx.doi.org/10.2307/3545044), 1992.

818 Harper, M. A., Howorth, R., and McLeod, M.: Late Holocene diatoms in Lake
819 Poukawa: Effects of airfall tephra and changes in depth, *New Zeal J Mar Fresh*,
820 20, 107-118, [10.1080/00288330.1986.9516135](http://dx.doi.org/10.1080/00288330.1986.9516135), 1986.

821 Hartmann, J., and Moosdorf, N.: The new global lithological map database GLiM:
822 A representation of rock properties at the Earth surface, *Geochem Geophys Geosy*,
823 13, 2012.

824 Hashimoto, I., and Jackson, M.: Rapid dissolution of allophane and kaolinite-
825 halloysite after dehydration, *Natl. Conf. on Clays and Clay Minerals*, 7th,
826 Washington, 1958, 102-113,

827 Heathcote, A., Ramstack Hobbs, J., Anderson, N. J., Frings, P., Engstrom, D., and
828 Downing, J.: Diatom floristic change and lake paleoproduction as evidence of

829 recent eutrophication in shallow lakes of the midwestern USA, *J Paleolimnol*, 1-
830 18, 10.1007/s10933-014-9804-4, 2014.

831 Heyng, A. M., Mayr, C., Lücke, A., Striewski, B., Wastegård, S., and Wissel, H.:
832 Environmental changes in northern New Zealand since the Middle Holocene
833 inferred from stable isotope records ($\delta^{15}\text{N}$, $\delta^{13}\text{C}$) of Lake Pupuke, *J Paleolimnol*,
834 48, 351-366, 10.1007/s10933-012-9606-5, 2012.

835 Hickman, M., and Reasoner, M. A.: Diatom responses to late Quaternary
836 vegetation and climate change, and to deposition of two tephras in an alpine and
837 a sub-alpine lake in Yoho National Park, British Columbia, *J Paleolimnol*, 11, 173-
838 188, 1994.

839 Hodder, A., Green, B., and Lowe, D.: A two-stage model for the formation of clay
840 minerals from tephra-derived volcanic glass, *Clay Miner*, 25, 313-327, 1990.

841 Hydes, D., and Liss, P.: Fluorimetric method for the determination of low
842 concentrations of dissolved aluminium in natural waters, *Analyst*, 101, 922-931,
843 1976.

844 ISSS-ISRIC-FAO: World Reference Base for Soil Resources, World Soil Resources
845 Reports, edited by: FAO, Rome, 1998.

846 Johansson, H., Lind, E.M. and Wastegård, S.: Proximal tephra glass geochemistry
847 from eruptions in the Azores archipelago and possible links with sites in Ireland,
848 The Holocene, submitted.

849 Johnson, T. C., Brown, E. T., and Shi, J.: Biogenic silica deposition in Lake Malawi,
850 East Africa over the past 150,000 years, *Palaeogeogr Palaeoclimatol*, 303, 103-109,
851 10.1016/j.palaeo.2010.01.024, 2011.

852 Kamatani, A., and Oku, O.: Measuring biogenic silica in marine sediments, *Mar
853 Chem*, 68, 219-229, 2000.

854 Kameník, J., Mizera, J., and Řanda, Z.: Chemical composition of plant silica
855 phytoliths, *Environ Chem Lett*, 11, 189-195, 10.1007/s10311-012-0396-9, 2013.

856 Koning, E., Epping, E., and Van Raaphorst, W.: Determining biogenic silica in
857 marine samples by tracking silicate and aluminium concentrations in alkaline
858 leaching solutions, *Aquat Geochem*, 8, 37-67, 2002.

859 Le Bas, M., Le Maitre, R., Streckeisen, A., and Zanettin, B.: A chemical classification
860 of volcanic rocks based on the total alkali-silica diagram, *J Petrol*, 27, 745-750,
861 1986.

862 Leinen, M.: Normative calculation technique for determining opal in deep-sea
863 sediments, *Geochim Cosmochim Acta*, 41, 671-676, 1977.

864 Levard, C., Doelsch, E., Basile-Doelsch, I., Abidin, Z., Miche, H., Masion, A., Rose, J.,
865 Borschneck, D., and Bottero, J. Y.: Structure and distribution of allophanes,
866 imogolite and proto-imogolite in volcanic soils, *Geoderma*, 183-184, 100-108,
867 10.1016/j.geoderma.2012.03.015, 2012.

868 Lind, E. M., and Wastegård, S.: Tephra horizons contemporary with short early
869 Holocene climate fluctuations: new results from the Faroe Islands, *Quatern Int*,
870 246, 157-167, 2011.

871 Lotter, A., Birks, H., and Zolitschka, B.: Late-glacial pollen and diatom changes in
872 response to two different environmental perturbations: volcanic eruption and
873 Younger Dryas cooling, *J Paleolimnol*, 14, 23-47, 1995.

874 Lowe, D. J.: Stratigraphy, age, composition, and correlation of late Quaternary
875 tephra interbedded with organic sediments in Waikato lakes, North Island, New
876 Zealand, *New Zealand journal of geology and geophysics*, 31, 125-165, 1988.

877 Lowe, D. J.: Tephrochronology and its application: A review, *Quat Geochronol*, 6,
878 107-153, 10.1016/j.quageo.2010.08.003, 2011.

879 Lyle, A. O., and Lyle, M.: Determination of biogenic opal in pelagic marine
880 sediments: a simple method revisited, *Proceedings of the Ocean Drilling*
881 *Program, Initial Reports*, 2002, 1-21,

882 Mackie, E. A., Davies, S. M., Turney, C. S., Dobbyn, K., Lowe, J. J., and Hill, P. G.: The
883 use of magnetic separation techniques to detect basaltic microtephra in last
884 glacial-interglacial transition (LGIT; 15–10 ka cal. bp) sediment sequences in
885 Scotland, *Scot J Geol*, 38, 21-30, 2002.

886 Melzer, S. E., Chadwick, O. A., Hartshorn, A. S., Khomo, L. M., Knapp, A. K., and
887 Kelly, E. F.: Lithologic controls on biogenic silica cycling in South African savanna
888 ecosystems, *Biogeochemistry*, 108, 317-334, 2012.

889 Meunier, J. D., Keller, C., Guntzer, F., Riotte, J., Braun, J. J., and Anupama, K.:
890 Assessment of the 1% Na₂CO₃ technique to quantify the phytolith pool,
891 *Geoderma*, 216, 30-35, 10.1016/j.geoderma.2013.10.014, 2014.

892 Meyer-Jacob, C., Vogel, H., Boxberg, F., Rosén, P., Weber, M. E., and Bindler, R.:
893 Independent measurement of biogenic silica in sediments by FTIR spectroscopy
894 and PLS regression, *Journal of Paleolimnology*, 52, 245-255, 2014.

895 Morley, D. W., Leng, M. J., Mackay, A. W., Sloane, H. J., Rioual, P., and Battarbee, R.
896 W.: Cleaning of lake sediment samples for diatom oxygen isotope analysis, *J*
897 *Paleolimnol*, 31, 391-401, 2004.

898 Müller, P., and Schneider, R.: An automated leaching method for the
899 determination of opal in sediments and particulate matter, *Deep-Sea Res PT I*,
900 40, 425-444, 1993.

901 Norrdahl, H., and Hafliðason, H.: The Skogar tephra, a Younger Dryas marker in
902 north Iceland, *Boreas*, 21, 23-41, 1992.

903 Oelkers, E. H., and Gislason, S. R.: The mechanism, rates and consequences of
904 basaltic glass dissolution: I. An experimental study of the dissolution rates of
905 basaltic glass as a function of aqueous Al, Si and oxalic acid concentration at 25 C
906 and pH= 3 and 11, *Geochim Cosmochim Ac*, 65, 3671-3681, 2001.

907 Ohlendorf, C., and Sturm, M.: A modified method for biogenic silica
908 determination, *Journal of Paleolimnology*, 39, 137-142, 2008.

909 Parfitt, R.: Allophane and imogolite: role in soil biogeochemical processes, *Clay*
910 *Miner*, 44, 135-155, 2009.

911 Pollard, A., Blockley, S., and Ward, K.: Chemical alteration of tephra in the
912 depositional environment: theoretical stability modelling, *J Quaternary Sci*, 18,
913 385-394, 2003.

- 914 Prokopenko, A. A., Hinnov, L. A., Williams, D. F., and Kuzmin, M. I.: Orbital forcing
915 of continental climate during the Pleistocene: a complete astronomically tuned
916 climatic record from Lake Baikal, SE Siberia, *Quaternary Sci Rev*, 25, 3431-3457,
917 2006.
- 918 Reyerson, P.: *Reactive Silica in Loess-Derived Soils of Central North America*,
919 *Doctor of Philosophy, Geography, University of Wisconsin-Madison*, 187 pp.,
920 2012.
- 921 Rose, N., Golding, P., and Battarbee, R.: Selective concentration and enumeration
922 of tephra shards from lake sediment cores, *The Holocene*, 6, 243-246, 1996.
- 923 Saccone, L., Conley, D., Koning, E., Sauer, D., Sommer, M., Kaczorek, D., Blecker, S.,
924 and Kelly, E.: Assessing the extraction and quantification of amorphous silica in
925 soils of forest and grassland ecosystems, *Eur J Soil Sci*, 58, 1446-1459, 2007.
- 926 Sauer, D., Saccone, L., Conley, D., Herrmann, L., and Sommer, M.: Review of
927 methodologies for extracting plant-available and amorphous Si from soils and
928 aquatic sediments, *Biogeochemistry*, 80, 89-108, 2006.
- 929 Sommer, M., Jochheim, H., Höhn, A., Breuer, J., Zagorski, Z., Busse, J., Barkusky, D.,
930 Meier, K., Puppe, D., and Wanner, M.: Si cycling in a forest biogeosystem—the
931 importance of transient state biogenic Si pools, *Biogeosciences*, 10, 4991-5007,
932 2013.
- 933 Stephens, J. C., and Hering, J. G.: Factors affecting the dissolution kinetics of
934 volcanic ash soils: dependencies on pH, CO₂, and oxalate, *Appl Geochem*, 19,
935 1217-1232, 2004.
- 936 Struyf, E., and Conley, D.: Emerging understanding of the ecosystem silica filter,
937 *Biogeochemistry*, 107, 9-18, 2012.
- 938 Telford, R. J., Barker, P., Metcalfe, S., and Newton, A.: Lacustrine responses to
939 tephra deposition: examples from Mexico, *Quaternary Sci Rev*, 23, 2337-2353,
940 2004.
- 941 Turney, C. S.: Extraction of rhyolitic component of Vedde microtephra from
942 minerogenic lake sediments, *J Paleolimnol*, 19, 199-206, 1998.
- 943 Unkel, I., Björck, S., and Wohlfarth, B.: Deglacial environmental changes on Isla de
944 los Estados (54.4 S), southeastern Tierra del Fuego, *Quaternary Sci Rev*, 27,
945 1541-1554, 2008.
- 946 Van Cappellen, P., Dixit, S., and van Beusekom, J.: Biogenic silica dissolution in the
947 oceans: Reconciling experimental and field - based dissolution rates, *Global*
948 *Biogeochem Cy*, 16, 23-21-23-10, 2002.
- 949 Van der Putten, N., Verbruggen, C., Björck, S., Michel, E., Disnar, J.-R., Chapron, E.,
950 Moine, B. N. and de Beaulieu, J.-L.: The Last Termination in the South Indian
951 Ocean: a unique terrestrial record from Kerguelen Islands (49°S) situated within
952 the Southern Hemisphere westerly belt, *Quaternary Science Reviews*,
953 10.1016/j.quascirev.2015.05.010, in press.
- 954 Verschuren, D., Johnson, T., Kling, H., Edgington, D., Leavitt, P., Brown, E., Talbot,
955 M., and Hecky, R.: History and timing of human impact on Lake Victoria, East
956 Africa, *Proc R Soc Lond B*, 269, 289-294, 2002.

- 957 Wastegård, S., Björck, S., Possnert, G., and Wohlfarth, B.: Evidence for the
958 occurrence of Vedde Ash in Sweden: radiocarbon and calendar age estimates, *J*
959 *Quaternary Sci*, 13, 271-274, 1998.
- 960 Wolff-Boenisch, D., Gislason, S. R., Oelkers, E. H., and Putnis, C. V.: The dissolution
961 rates of natural glasses as a function of their composition at pH 4 and 10.6, and
962 temperatures from 25 to 74 C, *Geochim Cosmochim Ac*, 68, 4843-4858, 2004.
- 963 Wulf, S., Ott, F., Słowiński, M., Noryskiewicz, A. M., Dräger, N., Martin-Puertas, C.,
964 Czymzik, M., Neugebauer, I., Dulski, P., and Bourne, A. J.: Tracing the Laacher See
965 Tephra in the varved sediment record of the Trzechowskie palaeolake in central
966 Northern Poland, *Quaternary Sci Rev*, 76, 129-139, 2013.

Table 1 The provenance, origin of the sample, eruption date and composition of the specific tephra deposits analyzed.

Tephra	Origin	Profile	Age[#]	Composition	Reference
Hekla1991	Iceland	Fresh deposit	1991 AD	Basaltic-Andesite	Gudmundsson et al. 1992
EFJ2010_SJV	Iceland	Fresh deposit	2010 AD	Trachy-andesite	Unpublished data ^a
EFJ2010_1504	Iceland	Fresh deposit	2010 AD	Trachy-andesite	Gislason et al 2011a&b.
Fogo A	Azores, Portugal	Buried Soil	c. 5000 cal BP	Trachyte	Johansson et al, subm. ^b
PAS-2T39	Argentina	Lake	48742 cal BP	Rhyolite	Wastegård et al. 2013
TC09_48a	Kerguelen Island	Buried Soil	c. 1000 cal BP	Trachyte	Unpublished data ^c
Pompeii	Italy	Buried Soil	79 AD	Tephri-phonolite	Unpublished data ^d
Vedde Ash	Iceland	Fresh deposit	12100 cal BP	Mixed Basalt and Rhyolite	Norrdahl & Hafliðason 1992 [§]
Reykjanes1226	Iceland	Soil	1226 AD	Basalt	Gísladóttir G. et al, 2010.
Cav-A	Azores, Portugal	Peat bog	1000 cal BP	Tephrite	Björck et al., 2006
Saksunarvatn	Faroe Island	Lake	10300 cal BP	Basalt	Lind & Wastegård, 2011 + Tephabase
Tuhua	New Zealand	Lake	7165 cal BP	Peralkaline Rhyolite	Heyng et al., 2012
Armor1000	Kerguelen Island	Peat bog	c. 1000 cal BP	Trachyte	Unpublished data ^e
Katla1500	Iceland	Soil	1500 AD	Basalt	Hafliðason et al., 1992
Reclus R₁	Argentina	Lake	15000 cal BP	Rhyolite	Unkel et al. 2008

[#]Reported ages expressed as calendar years (AD), calibrated ¹⁴C ages (cal BP; BP being 1950 AD by convention) and approximations based on unpublished radiocarbon dates; [§] Referred to as the Skógar Tephra

^a Surface grab sample collected shortly after 2010 eruption at the south side in Seljavellir (N63°34'; W19°37'), and stored dried, used data Gislason et al. 2011b for typical ash;^b Surface grab sample collected from the airfall deposit (N37°43'10.6; W25°30'0.96), stored dried. ^cSampled along a natural cut through the fluvial, volcano-sedimentary and peat deposits, at southeast of the Rallier du Baty Peninsula (S49°41'42" ; E68°57'55"), dry pumices were extracted from the ignimbrite deposit and stored dried. ^dSample taken during archaeological investigation of Pompeii, quarter VI.30, room 2 (N40° 45'; E14° 29'), stored dried. ^eThe Armor peat sequence (S49°27.872; E69°43.484) was sampled by drilling in CALYPSO PVC tubes (ϕ = 11.5 cm), and stored cold (4°C) before freeze dried.

Table 2 Comparison of Si_{Alk} (wt% $SiO_2 \pm$ stdev; n=5) of 14 selected tephra deposits for two commonly applied methods: 0.1M Na_2CO_3 based on mineral dissolution slope 3-5hrs and 20-24hrs and 0.5M NaOH. Note: Sample EFJ2010_1504 is not included.

Name Tephra	3-5h Na_2CO_3	20-24h Na_2CO_3	NaOH	$Si_{Alk,20-24h}/Si_{Alk,3-5h}$
Hekla1991	0.49±0.27	2.75	0.27	5.61
EFJ2010_SJV	0.30±0.15	2.14±0.25	0.30	7.13
Fogo A	0.91±0.29	2.66±0.23	1.68	2.92
PAS-2T39	1.35±0.31	4.82	2.32	3.57
TC09_48a	1.13±0.27	6.00	4.34	5.31
Pompeii	1.08±0.05	2.73±0.46	0.90	2.53
Reykjanes1226	1.31±0.40	0.87	2.30	0.66
Vedde Ash	1.54±0.41	3.86	1.86	2.51
Saksunarvatn	5.82±1.13	8.23	5.57	1.41
Cav-A	1.13±0.19	1.91	1.60	1.69
Tuhua	7.73±0.59	14.00	10.53	1.81
Armor1000	4.09±0.37	4.96±1.09	3.51	1.21
Katla1500	2.18±0.48	3.39±1.04	4.89	1.56
Reclus R₁	16.68±1.32	18.10	23.47	1.09

Table 3 Modeled dissolution parameters after alkaline (NaOH) extraction of untreated samples. For each fraction ($Si_{Alk,x}$; wt% SiO_2) the Si:Al_x ratios, rate of non-linear dissolution/release k_x (min^{-1}) for fraction x and b (wt% SiO_2 min^{-1}) the slope of the mineral dissolution with a Si:Al_{min} ratio are given for all samples. Additional column representing the Si and Al ratio of unweathered shards based on available EMPA data (Si:Al_{solid}).

Sample	Fraction 1			Fraction 2			Fraction 3			Mineral		Total	EMPA*
	$Si_{Alk,1}$	k_1	Si:Al ₁	$Si_{Alk,2}$	k_2	Si:Al ₂	$Si_{Alk,3}$	k_3	Si:Al ₃	b	Si:Al _{min}	$Si_{Alk,tot}$	Si:Al _{solid}
Hekla1991	0.27	0.45	4.03	0.032	3.25	0.27	3.35
EFJ2010_SJV	0.30	0.15	3.41	0.027	4.08	0.30	3.41
EFJ2010_1504	1.24	0.16	3.53	0.116	3.59	1.24	3.44
Fogo A	1.68	0.11	3.98	0.108	3.12	1.68	3.44
PAS 2T39	2.32	0.11	4.92	0.130	4.17	2.32	4.89
TC09_48a	3.58	0.05	3.59	0.76	1.01	0.95	.	.	.	0.188	3.57	4.34	3.86
Pompeii	0.45	0.23	1.19	0.45	1.77	2.17	.	.	.	0.041	1.58	0.90	2.35
Vedde Ash	0.90	0.11	1.73	0.96	0.94	4.40	.	.	.	0.057	3.54	1.86	3.94
Reykjanes1226	0.68	0.05	2.15	1.62	1.65	1.03	.	.	.	0.038	1.19	2.30	3.84
Saksunarvatn	2.15	0.21	2.31	3.42	1.89	3.55	.	.	.	0.057	3.71	5.57	3.31
Cav-A	0.58	0.05	8.00	1.02	1.05	0.46	.	.	.	0.017	2.13	1.60	2.97
Tuhua	8.01	0.14	26.26	2.52	0.74	22.40	.	.	.	0.201	8.71	10.53	7.21
Armor1000	2.89	0.19	26.83	0.61	1.12	0.37	.	.	.	0.079	4.31	3.51	3.58
Katla1500	2.01	0.16	13.42	2.88	0.46	0.91	.	.	.	0.038	2.36	4.89	3.57
Reclus R ₁	10.31	0.19	9.03	13.12	0.18	18.05	0.04	0.31	0.60	0.000	0.01	23.47	N/A

*Electron Microprobe Analysis data is based on available data (overview Table 1; Fig. 1).

Table 4 Modeled dissolution parameters after alkaline (NaOH) extraction of heavy liquid separated a) volcanic glass shards and b) biogenic silica fractions. For each fraction ($Si_{Alk,x}$; wt% SiO_2) the Si/ Al_x ratios, rate of non-linear dissolution/release k_x (min^{-1}) for fraction x and b (wt% SiO_2 min^{-1}) the slope of the mineral dissolution with a Si/ Al_{min} ratio are given for all samples.

Sample	Volcanic glass shards						Biogenic Si								
	Fraction 1			Mineral		Total	Fraction 1			Fraction 2			Mineral		Total
	$Si_{Alk,1}$	k_1	Si: Al_1	b	Si: Al_{min}	$Si_{Alk,tot}$	$Si_{Alk,1}$	k_1	Si: Al_1	$Si_{Alk,2}$	k_2	Si: Al_2	b	Si: Al_{min}	$Si_{Alk,tot}$
Hekla1991	3.45	0.58	20.08	0.049	1.92	3.45
EFJ2010_SJV	2.31	0.68	98.43	0.042	4.22	2.31
EFJ2010_1504	15.70	0.96	80.60	0.215	3.65	15.70
Vertical bFogo A	2.51	0.39	70.76	0.263	3.02	2.51
PAS 2T39	2.24	0.28	15.92	0.339	4.15	2.24
TC09_48a	1.25	0.65	42.51	0.294	3.81	1.25
Pompeii	22.59	0.90	110.64	0.027	1.45	22.59
Vedde Ash	0.54	1.27	657.58	0.031	3.78	0.54
Reykjanes1226	3.39	0.94	38.61	0.066	4.08	3.39
Saksunarvatn Cav-A	4.95	1.15	59.77	0.023	2.33	4.95	79.25	0.28	20504	79.25
Tuhua	3.84	0.19	17.00	0.206	6.59	3.84	23.50	0.47	390	30.38	0.05	7.50	.	.	53.88
Armor1000	1.82	0.43	371.55	0.097	2.53	1.82	79.78	0.37	361	79.78
Katla1500	4.60	0.97	37.72	0.095	3.33	4.60	66.66	0.90	155	.	.	.	0.063	4.37	66.66
Reclus R ₁	77.33	0.23	111	77.33

Figures:

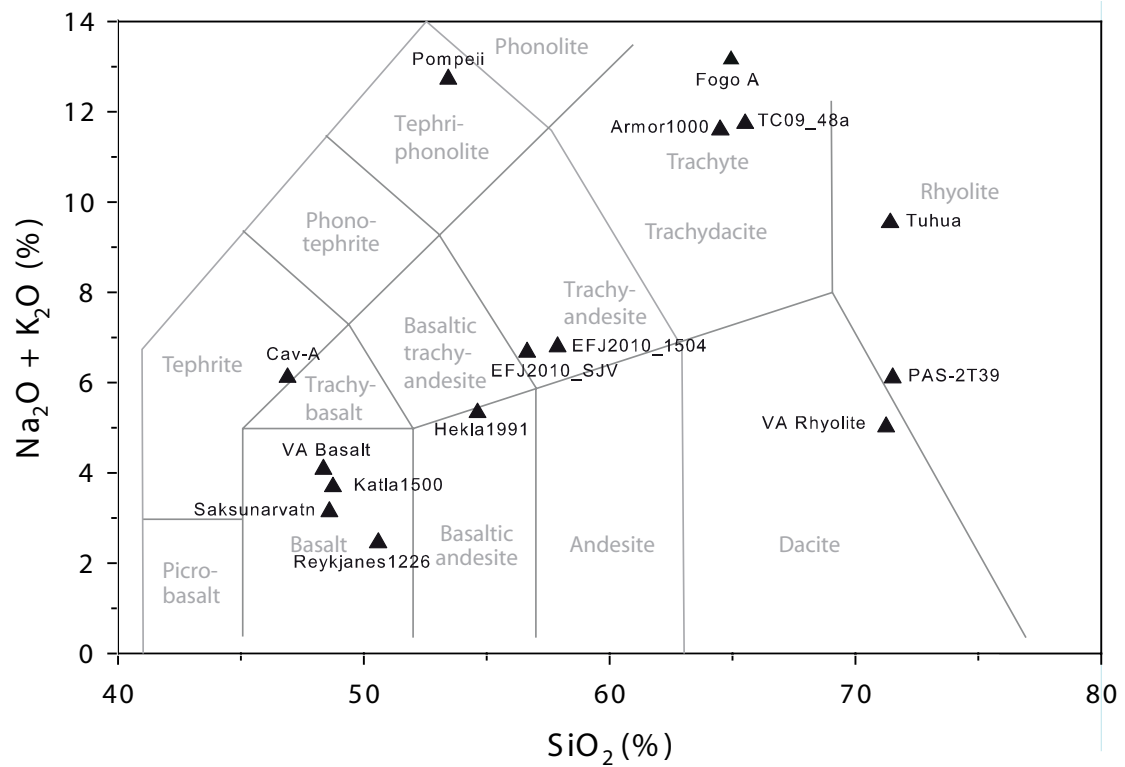


Figure 1 Composition of glass shards in our tephra samples presented on a total alkali silica diagram (SiO₂ vs. Na₂O +K₂O), a standard classification used for pyroclastic volcanic rocks based on non-genetic features. Geochemical boundaries are according to Le Bas et al. (1986). Data are normalized averages of EMPA analysis. No data are available for Reclus R₁ Sample

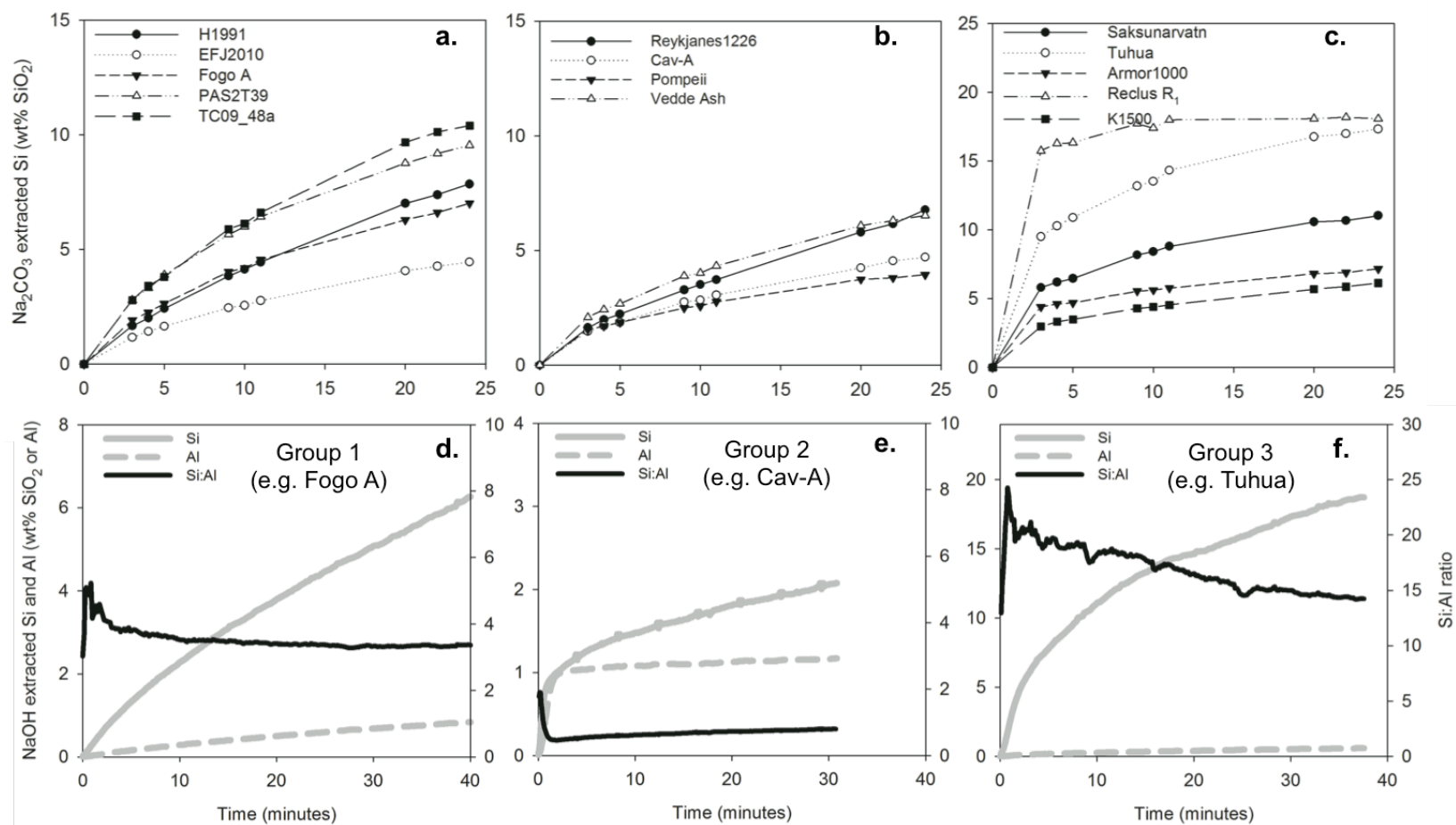


Figure 2 Dissolution curves of untreated tephra deposits grouped by characteristic features during the semi continuous extraction with Na_2CO_3 (a-c) for Si and continuous extraction NaOH (d-f) for Si, Al and Si:Al ratio. Note: Groups are the same between methods but time unit x-axis differs between a-c and d-f. For NaOH only 1 representative curve per group is presented Group 1 contains Hekla1991, both EFJ2010, Fogo A, PAS-2T39 and TC09_48a; Group 2 contains Reykjanes1226, Cav-A, Pompeii and Vedde Ash; Group 3 contains Saksunarvatn, Tuhua, Armor1000, Katla1500 and Reclus R₁.

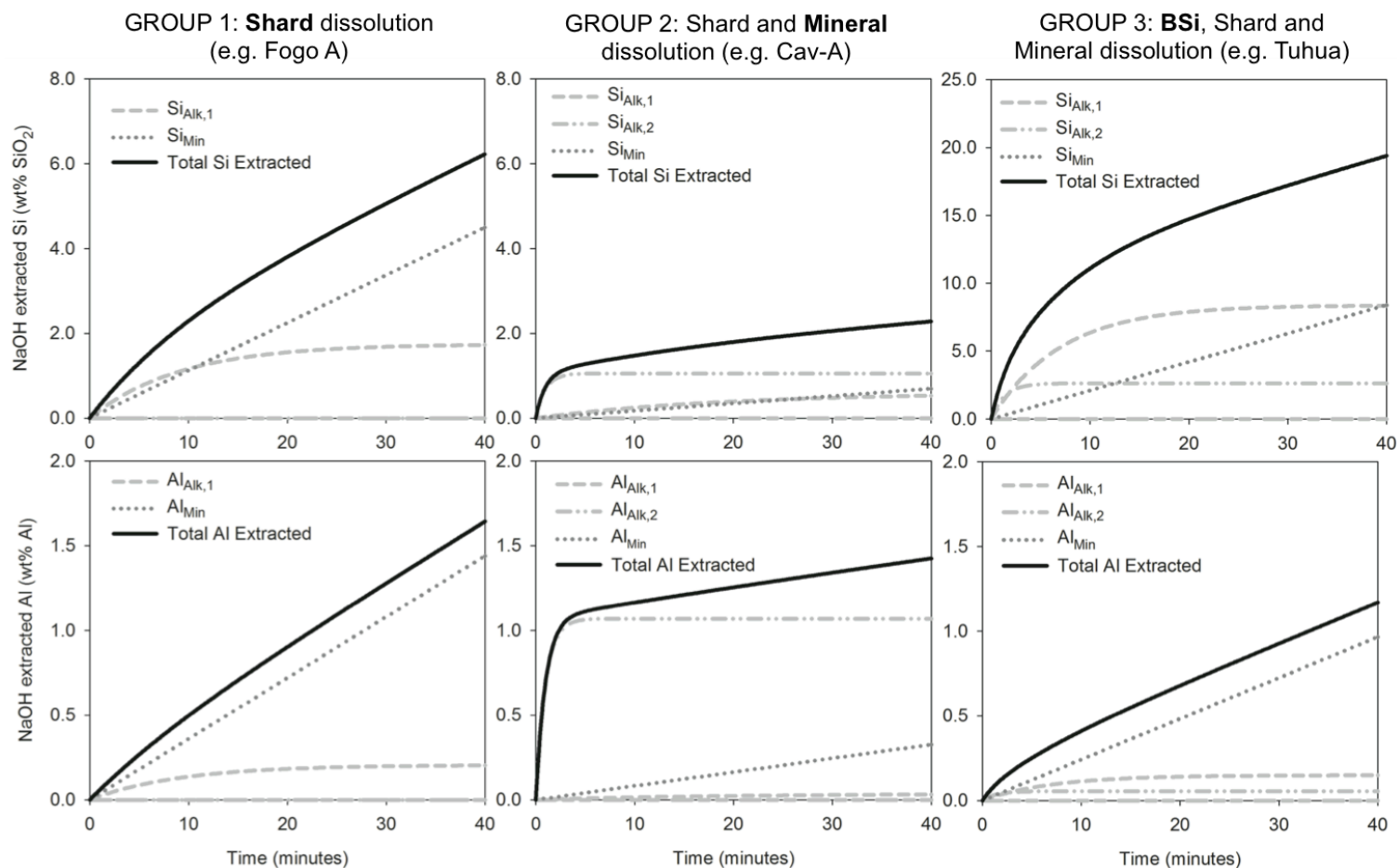


Figure 3 Separation in non-linear (Si_{Alk} & Al_{Alk}) and linear (Si_{Min} & Al_{Min}) fractions based modeling the continuous dissolution curves of Si and Al using Equation 1, grouped by their specific characteristics. Grouped by dominant fraction (in **bold**): Shards (solid circles), Minerals (open circles, i.e. nanocrystalline and clay minerals) or Biogenic Si (triangles). Group 1 contains Hekla1991, both EFJ2010, Fogo A PAS-2T39 and TC09_48a; Group 2 contains Reykjanes1226, Cav-A, Pompeii and Vedde Ash; Group 3 contains Saksunarvatn, Tuhua, Amor1000, Katla1500 and Reclus R₁.

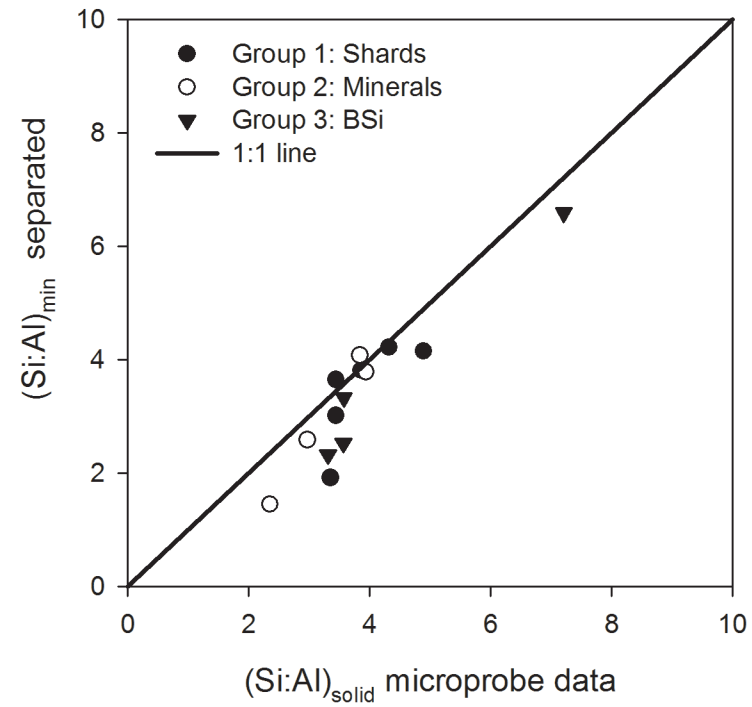
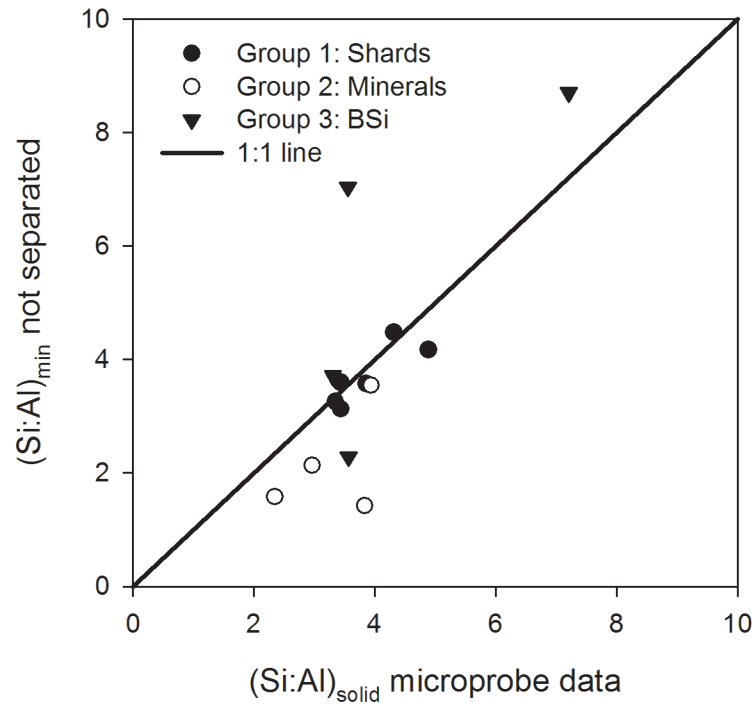


Figure 4 Comparison of $\text{Si:Al}_{\text{solid}}$ (from EMPA) and $\text{Si:Al}_{\text{min}}$ during alkaline dissolution (Table 3). Grouped by dominant fraction: Shards (solid circles), Minerals (open circles, i.e. nanocrystalline and clay minerals) or Biogenic Si (triangles). No data are available for Reclus R₁ Sample

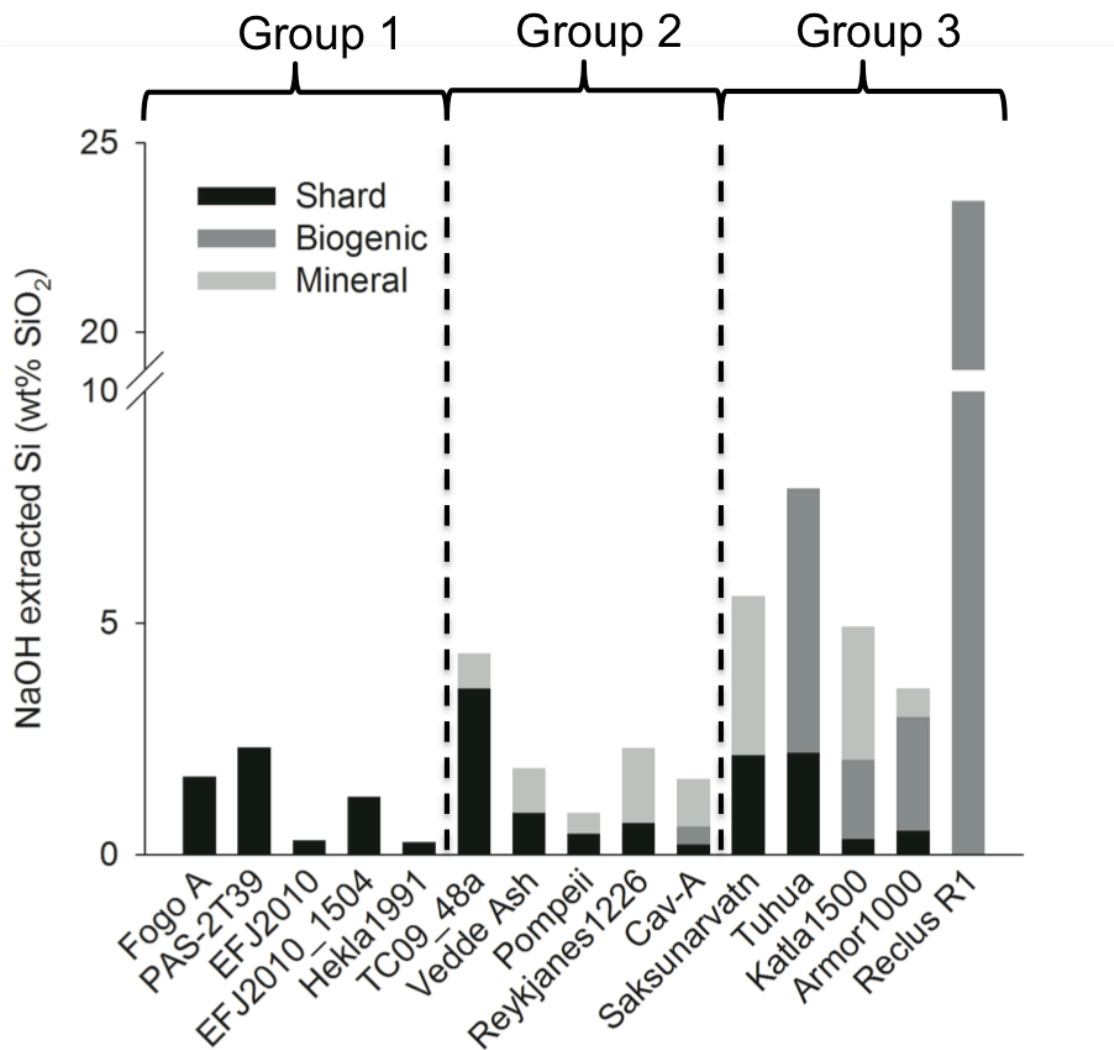


Figure 5 Separation of biogenic vs. non-biogenic (i.e. mineral or shard) fractions during alkaline extractions for all selected tephra deposits. Note: TC09_48a was reclassified to group 2 as it has a non-biogenic Si_{Alk} source.